Acta Cryst. (1995). **B51**, 31–36

Polymorphic Phase Transformation of Fe_4Al_{13} Causing Multiple Twinning with Decagonal Pseudo-Symmetry

M. Ellner

Max-Planck-Institut für Metallforschung, Institut für Werkstoffwissenchaft, Seestrasse 75,
D-70174 *Stuttgart, Germany*

(*Received* 14 *March* 1994; *accepted* 11 *July* 1994)

Abstract

The polymorphic phase transformation of alloys $Fe_{25}Al_{75}$–$Fe_{23}Al_{77}$ found recently by metallographical investigation was confirmed by X-ray diffraction. The high-temperature phase Fe_4Al_{13}(h) has an $oB\sim 50 = q$ unit cell, $a = 7.7510\,(9)$, $b = 4.0336\,(5)$ and $c = 23.771\,(3)$ Å, space group *Bmmm*, $c/a \simeq \tan 2\pi/5$. The low-temperature modification Fe_4Al_{13} (l) shows the structure of the Fe_4Al_{13} type [Black (1955*a*). *Acta Cryst.* **8**, 43–48]. A twinning model is discussed in reciprocal space for structures with the orthorhombic face-centred Bravais lattice having the axial ratio $c/a = \tan 2\pi/5$, *i.e.* the ratio $d_{002}/d_{101} = [(5)^{1/2} + 1]/2 = \tau$. Multiple-twinned Fe_4Al_{13} alloys yield diffraction patterns $(h0l)_q$ with decagonal pseudo-symmetry.

Introduction

The crystal structure of monoclinic Fe_4Al_{13} ($FeAl_3$), $mC(102-1.2)$, $C2/m$, $a = 15.489\,(1)$, $b = 8.0831\,(5)$, $c = 12.476\,(2)$ Å, $\beta = 107.72\,(2)^\circ$, was investigated by Black (1955*a*) by means of a special application of Patterson method sections. Weissenberg photographs, made by Black, taken with crystals oscillating about the twofold axis, showed that the crystals of Fe_4Al_{13} were twinned and that the twinning accentuates orthorhombic pseudo-symmetry. The diffraction spots were separated into two reciprocal lattices with a constant intensity ratio between their corresponding spots, and with their orientation related by a reflexion. This ratio was different for each crystal and some crystals exhibited more complicated multiples. Black's attempts to produce non-twinned crystals were not successful; therefore, twinned crystals were used for his structure determination. Recently, the structure of Fe_4Al_{13} was refined using a very small non-twinned crystal (Grin, Burkhardt, Ellner & Peters, 1994). The monoclinic space group $C2/m$ of Fe_4Al_{13}, as well as the general features of Black's structure (Black, 1955*a*), were confirmed. The shortest interatomic distances are Fe—Al 2.374, Fe—Fe 2.902 and Al—Al 2.533 Å (Black, 1955*b*): Fe—Al 2.257, Fe—Fe 2.906 and Al—Al 2.454 Å.

The type of Fe_4Al_{13}-twinning was also investigated by Black (1955*b*). The diffraction data showed that the twin components can be related in two ways, by reflexions across the (100) and (001) planes, or across planes perpendicular to these. Moreover, Black first discussed the possibility that the twinning can involve a translation (*e.g.* $a/2$ in the [100] direction). Using the high-resolution electron microscopy, planar defects as well as twinning with a glide component were observed recently in the sputtered Fe_4Al_{13} alloy by Tsuchimori, Ishimasa & Fukano (1992).

Contact twins of Fe_4Al_{13} on planes (100) and (001) were already observed by means of optical goniometry by Groth (1906). It was shown by Adam & Hogan (1975) that the growth of Fe_4Al_{13} lamellae follows the [010] direction. Ten-point stars were observed in aluminium-rich Fe–Al alloys prepared by rapid cooling; these stars were shown to be compatible with the twinning mechanism which occurs during the growth of Fe_4Al_{13} (Louis, Mora & Pastor, 1980). Using electron diffraction as well as transmission electron microscopy, tenfold twins were observed in an $Fe_{14}Al_{86}$ alloy (Fung *et al.*, 1986) and moreover, the coexistence of tenfold twins and decagonal quasicrystals in rapidly cooled Fe_4Al_{13} alloys was also observed by Fung, Zou & Yang (1987) and Zou, Fung & Kuo (1987).

Prismatic and twinned crystals were found in Ru_4Al_{13}, which is isotypical to Fe_4Al_{13} (Edshammar, 1965). The ternary representative of the structure type Fe_4Al_{13} – $Ni_3Zn_6Ga_4$ – showed a *conspicious twin formation* (Rajasekheran, Sarah & Schubert, 1982). Multiple twinning was observed not only in phases isotypical with Fe_4Al_{13}, but also in some homeotypical phases. The orthorhombic pseudo-symmetry of Co_4Al_{13} is accentuated by twinning (Hudd & Taylor, 1962). Finally, twinned crystals were found in Os_4Al_{13}, which structure is related to the Fe_4Al_{13} type (Edshammar, 1964).

Twinning may occur as a consequence of a phase transition from a higher to a lower symmetry phase; the twinned structures show higher (less negative) Gibbs free-energy variations than the untwinned structures (Salje, 1990, 1991). Recently, the polymorphic phase transformation of Fe_4Al_{13} was observed by means of optical microscopy with polarized light; further, hollow prismatic lamellae found in this alloy by means of scanning electron microscopy were interpreted as multiple-twinned crystals [repeated elbow twins (Ellner & Burkhardt, 1993)]. The aim of this study is to discuss the relationship between the high- and low-temperature modifications of Fe_4Al_{13} and to explain the polysynthetical twinning of Fe_4Al_{13}, which yields diffraction patterns showing decagonal pseudosymmetry, as found by Fung, Zou & Yang (1987) and Zou, Fung & Kuo (1987).

Experimental

Alloys (approximately 3 g) with the mole fraction $x_{Al} = 0.760$, $x_{Al} = 0.765$ and $x_{Al} = 0.770$ were prepared from iron (3mN8 Alfa Products) and aluminium (99.999% Heraeus) by melting in an arc furnace under argon at 60 kPa pressure (argon Messer–Griesheim 5.0). Because a significant weight loss of melted alloys was not observed, chemical analysis was not carried out. Bulk alloys were crushed after alloying and parts of each sample were used for the metallographical, X-ray diffraction and scanning electron microscopy investigations, as well as for a liquid quenching. The other parts were homogenized in corundum crucibles and encapsulated in evacuated silica tubes at 1373 K for 1 day. The bulk alloys were then powdered in mortar and heat-treated (1 h at 1073 K) for elimination of the internal stress.

For the splat-cooling, a shock-wave tube (Bucher, Ellner, Sommer & Predel, 1986) with argon (Messer-Griesheim 5.0) as well as a rotating propeller apparatus (Predel & Duddek, 1978) were used. Liquid-quenched as well as powdered and annealed alloys were used for X-ray investigations, employing a Guinier camera (Enraf–Nonius FR 552) with Co $K\alpha_1$, Fe $K\alpha_1$ and Cr $K\alpha_1$ radiation. Silicon-calibrated Guinier photographs were densitometrically analysed by a Line Scanner LS20 (KEJ Instruments). The lattice parameters were refined by least-squares.

Results

Guinier photographs with Co $K\alpha_1$ and Fe $K\alpha_1$ radiation of the heat-treated alloys $Fe_{23.5}Al_{76.5}$ and $Fe_{23}Al_{77}$ (bulk, 1 d, 1373 K; powder, 1 h, 1073 K) only contained diffraction lines of the Fe_4Al_{13} structure (Black, 1955*a*). Additional Fe_2Al_5 diffraction lines [Fe_2Al_5 type; Schubert, Rösler, Kluge, Anderko & Härle (1953)] were observed in the Guinier photographs of the annealed alloy $Fe_{24}Al_{76}$ (bulk, 1 d, 1373 K; powder, 1 h, 1073 K). On the other hand, Guinier photographs of the liquid-quenched alloys $Fe_{25}Al_{75}$–$Fe_{23}Al_{77}$ showed diffraction lines of a new phase closely related to the Fe_4Al_{13} structure. No difference in the diffraction patterns of the liquid-quenched alloys prepared in the rotating-wing apparatus and shock-wave tube was found. The diffraction lines of the new phase were indexed orthorhombically, $oB \sim 50$, $a = 7.7510\ (9)$, $b = 4.0336\ (5)$, $c = 23.771\ (3)$ Å, $c/a \simeq \tan 72° = \tan 2\pi/5$. The relationship between this $oB = q$ unit cell and Black's monoclinic unit cell of Fe_4Al_{13}(m) is

$$\begin{pmatrix} a \\ b \\ c \end{pmatrix}_q = \begin{pmatrix} \frac{1}{2} & 0 & 0 \\ 0 & \frac{1}{2} & 0 \\ \frac{1}{2} & 0 & 2 \end{pmatrix} \begin{pmatrix} a \\ b \\ c \end{pmatrix}_m. \qquad (1)$$

The orthorhombic modification of Fe_4Al_{13} is obviously a replacive high-temperature variant [Fe_4Al_{13}(h)] of the monoclinic low-temperature structure [Fe_4Al_{13}(l)]. This assumption can be supported by metallographical investigations with polarized light, showing a polymorphic phase transformation (Ellner & Burkhardt, 1993). No polymorphic phase transformation undergoes the neighbouring phase Fe_2Al_5. The powder diffraction data of Fe_4Al_{13}(h) ($Fe_{23.5}Al_{76.5}$, splat-cooled) are compared with the indexing for the closely related monoclinic low-temperature phase Fe_4Al_{13}(l), see Table 1.

The following diffraction lines were observed in the Guinier photographs of the liquid-quenched alloy $Fe_{23.5}Al_{76.5}$: hkl for $h + l = 2n$; $hk0$ for $h = 2n$; $0kl$ for $l = 2n$; $h0l$ for $h + l = 2n$; $00l$ for $l = 2n$; $h00$ for $h = 2n$. The possible space groups are *Bmmm* (standard setting *Cmmm*), *Bmm*2 (*Amm*2) and *Bm*2*m* (*Cmm*2). *Cmmm* is the minimal non-isomorphic supergroup of *C*2/*m*, which symmetry shows Black's monoclinic low-temperature phase Fe_4Al_{13}(l).

Discussion

The lattice geometry of Black's monoclinic low-temperature phase Fe_4Al_{13}(l) shows the following significant features:

(i) the axial ratio $c/a = \cos 36.34° \simeq [(5)^{1/2} + 1]/4 = \tau/2$;

(ii) the monoclinic angle $\beta \simeq 108° = 3\pi/5$, *i.e.* the supplementary angle between the a and c axis $\beta' \simeq 2\pi/5$.

The structural principle of monoclinic Fe_4Al_{13}(l) is based on one-dimensional channels built by icosahedra and/or pentagonal prisms (Grin, Burkhardt, Ellner & Peters, 1994).

Representatives of the Fe_4Al_{13}(l)-type also show similar lattice geometry: Ru_4Al_{13}, $c/a = \cos 36.59°$, $\beta = 107.77°$, and $Ni_3Zn_6Ga_4$, $c/a = \cos 36.17°$, $\beta = 108.05°$. It was recognized firstly by Henley (1985) that the layered structure of Fe_4Al_{13} can be

Table 1. *X-ray powder diffraction data for the high-temperature phase*

Fe_4Al_{13}(h), *oB* ~ 50 = *q*, *Bmmm*, *a* = 7.7510 (9), *b* = 4.0336 (5), *c* = 23.771 (3) Å, compared with the indexing $(hkl)_m$ for the low-temperature phase Fe_4Al_{13}(l), *mC*(102–1.2), *C*2/*m*, *a* = 15.489 (1), *b* = 8.0831 (5), *c* = 12.476 (2) Å, *β* = 107.72 (2)°. I_o, d_o = observed data; d_c = calculated data.

$(hkl)_g$	$(hkl)_m$	d_c (Å)	d_o (Å)	I_o
002	001	11.885	—	—
101	200, $\bar{2}01$	7.369	—	—
004	002	5.943	5.941	1
103	201, $\bar{2}02$	5.541	5.540	1
105	202, $\bar{2}03$	4.053	4.053	13
010	020	4.034	4.033	3
006	003	3.962	3.962	8
200	$\bar{4}01$	3.876	3.877	2
012	021	3.820	3.823	1
202	400, $\bar{4}02$	3.685	3.686	21
111	220, $\bar{2}21$	3.538	3.540	19
014	022	3.337	3.338	8
113	221, $\bar{2}22$	3.261	3.263	9
204	401, $\bar{4}03$	3.246	3.246	2
107	203, $\bar{2}04$	3.110	3.110	1
008	004	2.9714	2.9712	1
115	222, $\bar{2}23$	2.8589	—	—
016	023	2.8265	—	—
210	$\bar{4}21$	2.7946		—
206	402, $\bar{4}04$	2.7704	2.7719	1
212	420, $\bar{4}22$	2.7204	2.7200	1
301	$\bar{6}01$, $\bar{6}02$	2.5685	2.5672	1
214	421, $\bar{4}23$	2.5289	2.5291	5
109	204, $\bar{2}05$	2.5000	—	
117	223, $\bar{2}24$	2.4631	2.4638	4
303	600, $\bar{6}03$	2.4564	&	&
018	024	2.3923	2.3938	1
0,0,10	005	2.3771	—	—
208	403, $\bar{4}05$	2.3581	2.3529	3
216	422, $\bar{4}24$	2.2836	2.2850	1
305	601, $\bar{6}04$	2.2701	2.2606	2
311	$\bar{6}21$, $\bar{6}22$	2.1666	2.1660	2
119	224, $\bar{2}25$	2.1250	—	
313	620, $\bar{6}23$	2.0980	2.0982	100
1,0,11	205, $\bar{2}06$	2.0816	2.0814	21
307	602, $\bar{6}05$	2.0562	2.0557	13
0,1,10	025	2.0479	2.0482	34
218	423, $\bar{4}25$	2.0357	2.0356	53
2,0,10	404, $\bar{4}06$	2.0263	—	—
020	040	2.0168	2.0162	21
022	041	1.9884	1.9888	1
0,0,12	006	1.9809	1.9798	4
315	621, $\bar{6}24$	1.9783	—	
121	240, $\bar{2}41$	1.9453	—	—
400	$\bar{8}02$	1.9378	1.9377	15
402	$\bar{8}01$, $\bar{8}03$	1.9125	—	—
024	042	1.9098	—	—
123	241, $\bar{2}42$	1.8952	—	—
1,1,11	225, $\bar{2}26$	1.8498	—	—
309	603, $\bar{6}06$	1.8469	—	—
404	800, $\bar{8}04$	1.8423	—	—
317	622, $\bar{6}25$	1.8319	1.8320	1
2,1,10	424, $4\bar{2}6$	1.8107	—	—
125	242, $\bar{2}43$	1.8056	1.8050	1

decomposed into the rhombic tiles of the two-dimensional Penrose tiling.

The lattice geometry of the orthorhombic high-temperature phase Fe_4Al_{13}(h) is significant too: the axial ratio $c/a \simeq \tan 2\pi/5$. The unit cell of this high-temperature modification is closely related to that of the *hypersymmetric* layered structure $Ni_4Mn_{11}Al_{60}$, *oB*156, *Bbmm*, *a* = 23.8, *b* = 12.5, *c* = 7.55 Å, *a*/*c* = tan 72.4° (Robinson, 1954), as well as to the T_3 phase (MnZnAl); *oC*152, *Cmcm*, *a* = 7.78, *b* = 23.8, *c* = 12.6 Å, *b*/*a* = tan 71.9° (Damjanovic, 1961). For another homeotypical structure $Mn_3Cu_2Al_{20}$, *oB*150, *a* = 24.11, *b* = 12.51, *c* = 7.71 Å, *a*/*c* = tan 72.3°, reflexion twinning on {101} was observed (Robinson, 1952).

Analogous reflexion twins on {110}, exhibiting in electron diffraction patterns tenfold pseudo-symmetry, were observed for liquid-quenched NiZr (CrB type), *Cmcm*, *a* = 3.268, *b* = 9.937, *c* = 4.101 Å, *b*/*a* = tan 71.8° (Jiang, Hei, Guo & Kuo, 1985). *Pseudo-tenfold* twins were also observed in the metastable phase Cr_3C_{2-x} produced by crystallization of amorphous Cr–C alloys. This metastable phase is isotypical with Re_3B, *Cmcm*, *a* = 2.85, *b* = 9.26, *c* = 6.96 Å, *b*/*a* = tan 72.9°, and exhibits twinning on {110} (Bouzy, Le Caer & Bauer-Grosse, 1991).

Metallographical investigations with polarized light showed that the Fe_4Al_{13}(l) hollow prismatic lamellae are not true single crystals; they are formed by a domain-twinned microstructure. In direct space, a model was suggested for the twinned monoclinic Fe_4Al_{13}(l) modification (Ellner & Burkhardt, 1993), which proves that a statistical distribution of reflexion twinning on $(100)_m$, $(001)_m$ and $(\bar{2}01)_m$ yields five discrete orientations of the monoclinic Fe_4Al_{13}(l) unit cell. These five Fe_4Al_{13}(l) unit-cell positions differ in their orientation by 2π/5 rotation; at the same time they show parallel orientation of the [010] direction (repeated elbow twinning; Phillips, 1971).

This model is in general valid for the monoclinic structures with lattice geometry given by the axial

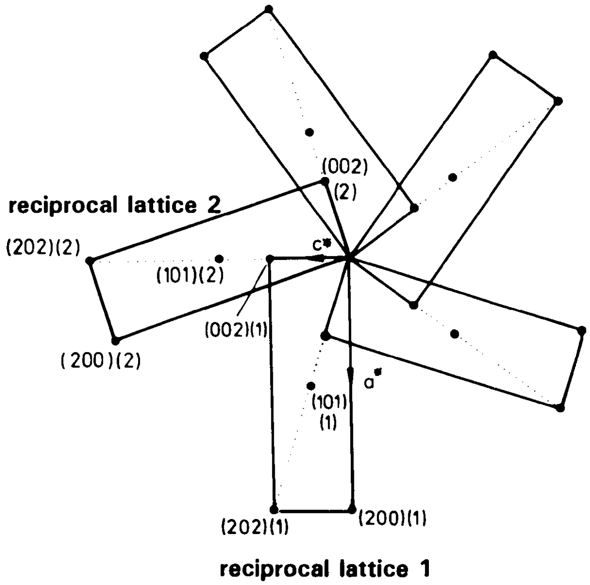

Fig. 1. Five *oB* reciprocal lattices ($a^*/c^* = \tan 2\pi/5$) with the common b^* axis rotated by an angle of 2π/5.

ratio $c/a = \cos 2\pi/10$ and the monoclinic angle $\beta = 3\pi/5$ (*i.e.* the supplementary unit-cell angle $\beta' = 2\pi/5$). The fact that planes of different zones $[(100)_m, (001)_m$ and $(\bar{2}01)_m]$ are situated parallel as a result of the repeated reflexion twinning is physically important; using the diffraction technique, the reflexions of these planes therefore lie on the same 'zone axis' (central line).

The reason for the twinning of the low-temperature phase is the displacive polymorphic phase transformation $Fe_4Al_{13}(h) \rightarrow Fe_4Al_{13}(l)$. The lattice geometry changes as a result of this phase transformation by slow lattice distortion. The pseudo-pentagonal lattice geometry of the high-temperature phase given by the axial ratio $c_q/a_q = \tan 2\pi/5$ becomes *nearly* pseudo-pentagonal in the low-temperature modification ($c_m/a_m \sim \cos 2\pi/10$).

Concerning the relationship between $Fe_4Al_{13}(h)$ and $Fe_4Al_{13}(l)$ (1), the twin planes $(100)_m$, $(001)_m$ and $(\bar{2}01)_m$ of the monoclinic unit cell (m) are analogous to the twin planes $(101)_q$, $(001)_q$ and $(\bar{1}01)_q$ of the orthorhombic unit cell (q), respectively. A characteristic feature accentuating the twinning process is the slight change in the value $d_{101} = 7.369$ Å of the high-temperature phase (q) in the metrically closely related values $d_{200} = 7.377$ and $d_{201} = 7.350$ Å (Black, 1955*a*,*b*) [$d_{200} = 7.380$ and $d_{201} = 7.349$ Å, respectively; Grin, Burkhardt, Ellner & Peters (1994)] of the low-temperature phase (m).

The reflexion twinning on $(101)_q$ causes a mirror image of the oB-$Fe_4Al_{13}(h)$ unit cell with the $2\pi/10$ rotation. A following reflexion twinning of this mirror image [as well as of the similarly oriented $Fe_4Al_{13}(h)$ unit cells] results in the $2\pi/5$ rotation of the initial $Fe_4Al_{13}(h)$ unit cell. It is plausible that this

$$\overline{ME} = S_{10} = 2c^* = \frac{1}{d_{(002)(2)}}$$

$$\overline{MC} = \sqrt{a^{*2} + c^{*2}} = \frac{1}{d_{(101)(1)}}$$

$$\frac{\overline{MC}}{\overline{ME}} = \tau = \frac{d_{(002)(2)}}{d_{(101)(1)}}$$

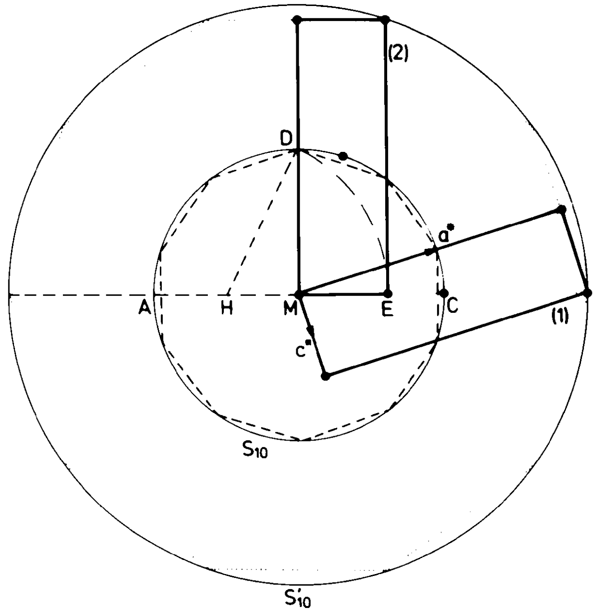

Fig. 2. Two oB reciprocal lattices ($a^*/c^* = \tan 2\pi/5$) with the common b^* axis incorporated in the geometrical golden-mean construction.

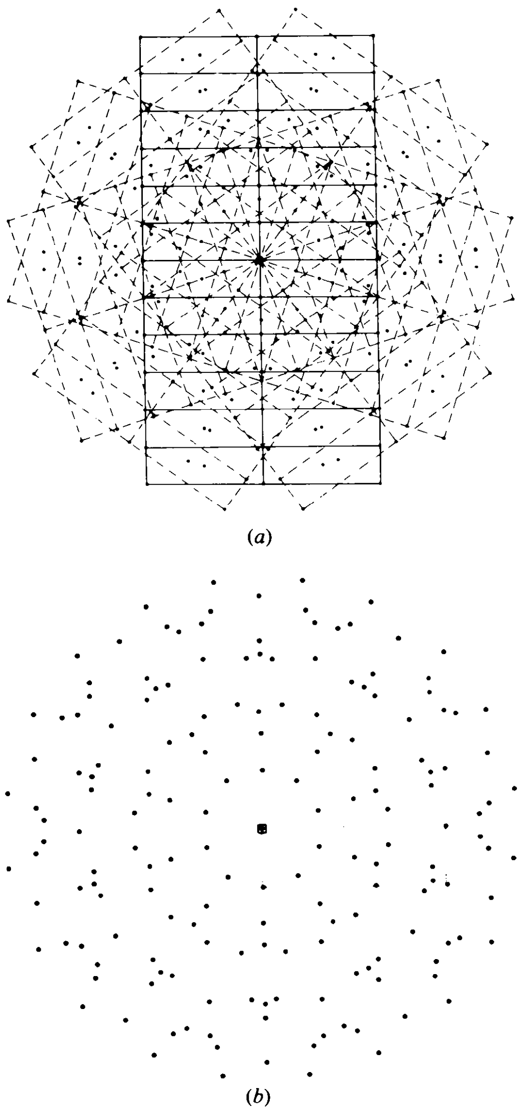
(*a*)

(*b*)

Fig. 3. (*a*) The ($h0l$) reciprocal space section through the network based on the five oB reciprocal lattice systems ($a^*/c^* = \tan 2\pi/5$) rotated about the [010] direction by an angle of $2\pi/5$. (*b*) The configuration of the lattice points from the ($h0l$) reciprocal space section shown in Fig. 3(*a*) exhibits decagonal pseudo-symmetry.

process can be repeated five times to obtain the initial *oB* unit-cell position.

The twinning model for the orthorhombic face-centred (*oB*, *oA*, *oC*) unit cells with the axial ratio $c/a = \tan 2\pi/5$ (b/c, $b/a = \tan 2\pi/5$) can also be used in reciprocal space. The type of face-centring of the orthorhombic Bravais lattice (*B*, *A* or *C*) does not change in reciprocal space; the axial ratios show the reciprocal values.

Five *oB* reciprocal lattices with the axial ratio $a^*/c^* = \tan 2\pi/5$ and the common axis b^* differing by the rotation angle $2\pi/5$ are presented in Fig. 1. This scheme shows the significant fact that two different zone reflexions, *e.g.* ($h0h$) of the reciprocal lattice (2) and ($00l$: $l = 2n$) of the reciprocal lattice (1), are situated on the common zone axis as a result of the repeated reflexion twinning on the (101) plane in direct space.

Two *oB* reciprocal lattices with the axial ratio $a^*/c^* = \tan 2\pi/5$ and the common axis b^* are incorporated in the classical geometric *golden-mean* construction in Fig. 2. These reciprocal lattices (1) and (2) differ in rotation by the angle $2\pi/5$. According to the geometrical golden-mean construction, the distance ratio $\overline{MC}/\overline{ME} = \tau$. Because of the distance $\overline{ME} = 1/d_{002}$ and the distance $\overline{MC} = 1/d_{101}$, the interplanar spacing ratio $d_{002}/d_{101} = \tau$ also [*cf.* the *d*-value ratio for $(002)_q$ and $(101)_q$ in Table 1].†

A network of five twinned *oB* reciprocal lattice systems ($a^*/c^* = \tan 2\pi/5$) with parallel direction [010] is given in Fig. 3(*a*). The reciprocal lattices also differ in orientation by the angle $2\pi/5$. The configuration of the corresponding lattice points without the network is displayed in Fig. 3(*b*). It is evident that this motif shows decagonal pseudo-symmetry. These reciprocal lattice points conform with the ($h0l$) diffraction pattern of a multiple-twinned structure with the *oB* ($c/a = \tan 2\pi/5$) or the monoclinic ($c/a = \cos 2\pi/10$, $\beta = 3\pi/5$) unit cell. A similar diffraction pattern is also the result of the microcrystalline domain structure with a statistical distribution of five discrete orientations of the *oB* unit cell in direct space (*e.g.* Fig. 18 in Ellner & Burkhardt, 1993).

Using the five *oB* reciprocal lattices which show geometry as quoted above, a characteristic share of the ($h0l$) reciprocal space section was indexed (Fig. 4). The number in brackets at the index $h0l$ indicates the corresponding *oB* reciprocal lattice. It can be seen that two kinds of relations between the reflexions situated on the zone axes can be found in this scheme:

(i) collinear reflexions corresponding to the same reciprocal lattice, *e.g.* (002) (3), (004) (3), (006) (3) *etc.*;

(ii) golden-mean relationship between the two coincident $\{h0h\}$ reflexions [(101) (1) + ($\bar{1}$01) (5); (202) (1) + ($\bar{2}$02) (5) *etc.*] on the one hand and the $\{001\}$ ($l = 2n$) reflexions [(002) (3); (004) (3) *etc.*] on the other.

Indexing of the ($h0l$) reciprocal space section shown in Fig. 4 was applied on the tenfold electron-diffraction patterns of the rapidly cooled alloy Fe_4Al_{13} observed by Fung, Zou & Yang (1987). This electron diffraction pattern is shown in Fig. 5.† Indexing given in Fig. 2(*a*) of the paper by Fung, Zou & Yang (1987) for the non-twinned Fe_4Al_{13} is based on Black's *mC*(102–1.2) unit cell. Concerning (1), there is full conformity between this and the indexing used for the high-temperature unit cell of Fe_4Al_{13}(h) ($oB \sim 50$) shown in Fig. 5.

---

† The mathematical proof has been deposited with the IUCr (Reference: JS0001). Copies may be obtained through The Managing Editor, International Union of Crystallography, 5 Abbey Square, Chester CH1 2HU, England.

† Reproduced courtesy of Taylor & Francis Ltd., London.

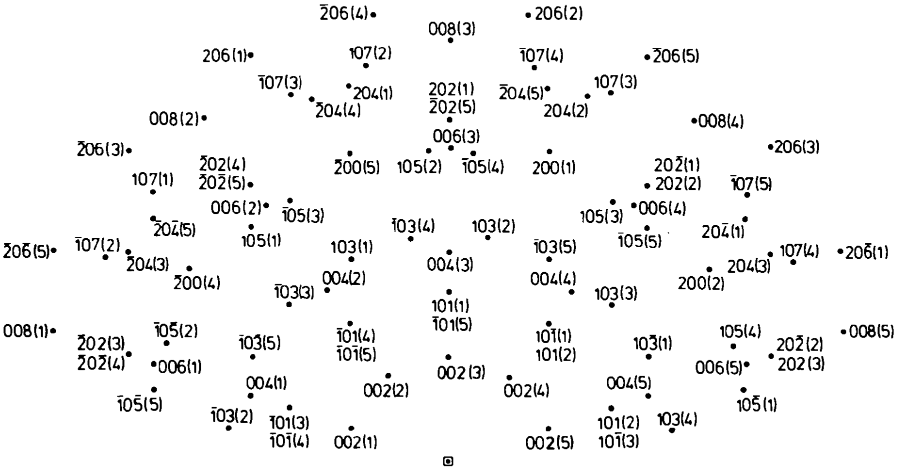

Fig. 4. An example of indexing of the lattice points from the ($h0l$) reciprocal space section shown in Fig. 3(*a*). The number in brackets (1–5) at the index $h0l$ indicates the corresponding *oB* reciprocal lattice.

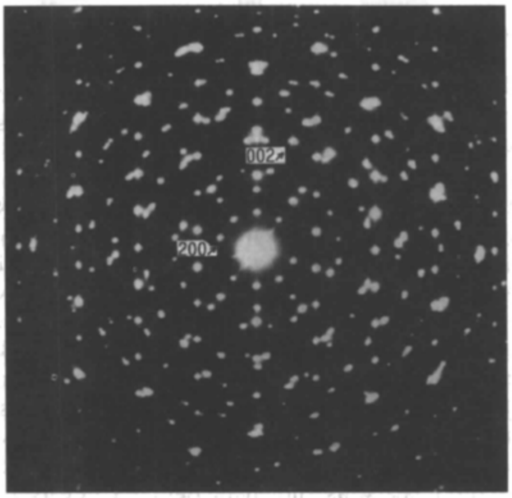

Fig. 5. Tenfold electron-diffraction pattern of the rapidly cooled alloy Fe_4Al_{13} observed by Fung, Zou & Yang (1987); reproduced courtesy of Francis & Taylor Ltd., London. Indexed are the lattice points of the high-temperature phase Fe_4Al_{13}(h), $oB \sim 50$, $a^*/c^* = \tan 2\pi/5$.

The distribution of the reciprocal lattice points in Fig. 4 presumes the regular 1/5 volume share of each oB unit-cell orientation. Intensity irregularities observed in Fig. 5 can be explained, apart from the absorption effect, by the unequal presence of the five possible oB unit-cell orientations in direct space.

This work was supported by Deutsche Forschungsgemeinschaft.

References

Adam, C. McL. & Hogan, L. M. (1975). *Acta Metall.* **23**, 345–354.

Black, P. J. (1955*a*). *Acta Cryst.* **8**, 43–48.

Black, P. J. (1955*b*). *Acta Cryst.* **8**, 175–181.

Bouzy, E., Le Caer, G. & Bauer-Grosse, E. (1991). *Phil. Mag. Lett.* **64**, 1–6.

Bucher, G., Ellner, M., Sommer, F. & Predel, B. (1986). *Mh. Chem.* **117**, 1367–1378.

Damjanovic, A. (1961). *Acta Cryst.* **14**, 982–987.

Edshammar, L.-E. (1964). *Acta Chem. Scand.* **18**, 2294–2302.

Edshammar, L.-E. (1965). *Acta Chem. Scand.* **19**, 2124–2130.

Ellner, M. & Burkhardt, U. (1993). *J. Alloys Compd.* **198**, 91–100.

Fung, K. K., Yang, C. Y., Zhou, Y. Q., Zhao, J. G., Zhan, W. S. & Shen, B. G. (1986). *Phys. Rev. Lett.* **56**, 2060–2063.

Fung, K. K., Zou, X. D. & Yang, C. Y. (1987). *Phil. Mag. Lett.* **55**, 27–32.

Grin, J., Burkhardt, U., Ellner, M. & Peters, K. (1994). *Z. Kristallogr.* **209**, 479–487.

Groth, P. (1906). *Chemische Krystallographie*, Erster Teil, pp. 47–48. Leipzig: Verlag von Wilhelm Engelmann.

Henley, C. L. (1985). *J. Non-Cryst. Solids*, **75**, 91–96.

Hudd, R. C. & Taylor, W. H. (1962). *Acta Cryst.* **15**, 441–442.

Jiang, W. J., Hei, Z. K., Guo, Y. X. & Kuo, K. H. (1985). *Phil. Mag. A*, **52**, L53–L58.

Lee, J. R. (1960). *J. Iron Steel Inst.* **194**, 222–224.

Louis, E., Mora, R. & Pastor, J. (1980). *Met. Sci.* **14**, 591–593.

Phillips, F. C. (1971). *An Introduction to Crystallography*, 4th ed., p. 186. London: Longman.

Predel, B. & Duddek, G. (1978). *Z. Metallkd.* **69**, 773–776.

Rajasekheran, T., Sarah, N. & Schubert, K. (1982). *Z. Metallkd.* **73**, 526–529.

Robinson, K. (1952). *Phil. Mag.* **43**, 775–782.

Robinson, K. (1954). *Acta Cryst.* **7**, 494–497.

Salje, E. K. H. (1990). *Phase Transitions in Ferroelastic and Co-Elastic Crystals.* Cambridge: Cambridge University Press.

Salje, E. K. H. (1991). *Acta Cryst.* A**47**, 453–469.

Schubert, K., Rösler, U., Kluge, M., Anderko, K. & Härle, L. (1953). *Naturwissenschaften*, **40**, 437.

Tsuchimori, M., Ishimasa, T. & Fukano, Y. (1992). *Phil. Mag. B*, **66**, 89–108.

Zou, X. D., Fung, K. K. & Kuo, K. H. (1987). *Phys. Rev. B*, **35**, 4526–4528.

Acta Cryst. (1995). B**51**, 36–43

A Family of τ-Inflated Monoclinic $Al_{13}Co_4$ Phases

By X. L. Ma, X. Z. Li and K. H. Kuo*

Beijing Laboratory of Electron Microscopy, Chinese Academy of Sciences, PO Box 2724, 100080 *Beijing, People's Republic of China*

(*Received* 25 *June* 1994; *accepted* 30 *August* 1994)

Abstract

Monoclinic τ^2-$Al_{13}Co_4$, τ^3-$Al_{13}Co_4$ and τ^4-$Al_{13}Co_4$ phases with a and c parameters about τ^2, τ^3 and τ^4 times [$\tau = (1 + 5^{1/2})/2 = 1.61803$, which is the golden number], respectively, greater than their counterparts in $Al_{13}Co_4$ (space group Cm, $a = 1.5183$, $b = 0.8122$, $c = 1.2340$ nm, $\beta = 107°54'$ [Hudd & Taylor (1962). *Acta Cryst.* **15**, 441–442]) have been found by selected-area electron diffraction and high-resolution electron

---

* Please send all correspondence to Dr K. H. Kuo, PO Box 2724, 100080 Beijing, People's Republic of China.